DUCTILITY OF ADHESIVELY BONDED TIMBER JOINTS

M. ANGELIDI, A. P. VASSILOPOULOS & T. KELLER
Composite Construction Laboratory (CCLab), Ecole Polytechnique Fédérale de Lausanne EPFL, Switzerland.

ABSTRACT

In the field of timber engineering, adhesive bonding remains a promising, though poorly developed, joining technique that may increase the structural stiffness and capacity of timber joints and structures. Selecting ductile adhesives may further allow to conceive ductile joints, which can compensate for the missing material ductility of timber. To demonstrate the potential of this approach, adhesively bonded double-lap timber joints were manufactured using a ductile acrylic adhesive and then subjected to axial tension and compression. The load–displacement responses were captured and compared to those of the same joints composed of a brittle epoxy adhesive. The effect of the different adhesives on the joint ductility has been studied and quantified.

Keywords: acrylics, adhesives, capacity, ductility, epoxy, spruce, stiffness, timber joint.

1 INTRODUCTION

Joints represent the most critical elements in the majority of timber structures; basically they can be conceived as mechanical or adhesively bonded joints. Bonded joints can exhibit higher efficiency than bolted ones due to a more uniform stress distribution [1, 2]; in the latter, high stress concentrations occur and the cross section is reduced [3]. In addition to the higher capacity of bonded joints, the stiffness is increased, the weight-to-strength ratio is reduced and fatigue strength and durability are improved; the latter due to the sealing by the adhesive [4]. Many different types of adhesives can be applied, depending on the targeted application.

One of the most important characteristic of load-bearing structures is ductility, i.e. the ability of a material or a structure to sustain inelastic deformation prior to failure, without loss of resistance. In redundant systems the internal forces can be redistributed, the energy from any impact or seismic actions can be dissipated and large deformations prior to failure can provide sufficient warning [5]. This issue of ductility is even more important when using brittle components, such as composite materials or wood, as in the case of this study. For this reason, ductile adhesives [6] are of special interest for creating ductile joints, and thus, compensate for the missing material ductility.

The basic definition of ductility is expressed as the ratio between the total and yield deformations of a material or joint [7]. However, a ductile behavior cannot always be derived only based on the non-linear response: in an elastically buckling member, for example, the unloading path follows the same non-linear path as the loading and no permanent deformation or related ductility are developed. Therefore, extended energy-based definitions of ductility, taking into account the dissipated inelastic energy during loading, were developed. The total energy, E_{tot}, corresponds to the total area under the load–displacement curve and is composed of the elastic energy, E_{el}, which is released while unloading and the dissipated inelastic one, E_{inel}, represented by the area between the loading and unloading path, respectively [8, 9]. Such energy-based definitions usually consider different ratios of these energies, i.e. E_{inel}/E_{tot} [10, 11] or E_{tot}/E_{el} [12].

The use of ductile adhesive joints to introduce ductility has already been performed in the case of brittle composite components [2]. However, a systematic and comprehensive study of the application of ductile adhesives for timber joints has not yet been performed, only a preliminary study concerning the load capacity is available [13]. The aim of this study is thus to

conceive such ductile adhesive joints and compare their performance in tension and compression (regarding stiffness, capacity and mode of failure) with similar joints composed of a brittle adhesive.

2 EXPERIMENTAL SETUP

2.1 Material and specimen fabrication

The experimental program in this study included a series of adhesively bonded double-lap timber joints, shaped in the dog-bone form, in order to prevent premature failure at the supports' area from the clamping of the specimens into the machine. The wood used for the fabrication of these joints was Norway spruce wood, belonging to the species of *Picea abies*, as it is one of the most widely used types of wood for structural applications by the timber industry. The wooden adherends were cut from clear logs of spruce wood, avoiding any obvious defects, such as notches, which could result in false interpretation of the material's behavior. For the assembling of these adherends, two kind of structural adhesives were used and two series of joints were manufactured: the first one using a brittle epoxy adhesive, Sika-Dur330, and the second one using a ductile and fast-curing acrylic adhesive, SikaFast5221NT; both adhesives were obtained from Sika AG, Switzerland [14, 15]. The ductile behavior of the acrylic adhesive has already been investigated and quantified in a previous work [16]. The basic mechanical properties of the materials used for the joints are summarized in Table 1.

The joint specimen's geometry is shown in Figure 1; the total length and width were 970 and 50 mm, respectively, and the thickness of the adhesive layer was 2 and 3 mm, for epoxy and acrylic joints, respectively. In the latter case, a thin layer of epoxy of 0.5 mm has been added between the wood and acrylic adhesive to improve the adhesion. The joints were fabricated under ambient laboratory conditions (21°C ± 3°C and 38% ± 10% relative humidity)

Table 1: Basic material mechanical properties [[1]2, [2]17, [3]18, [4]19, [5]14, [6]15, [7]measured].

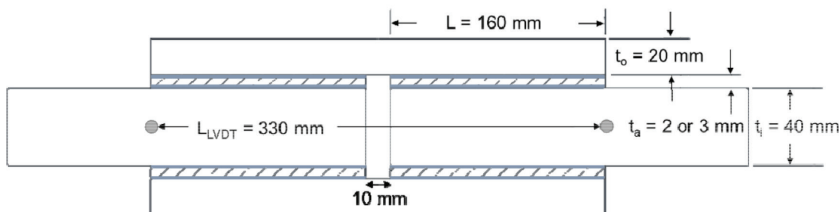| Material	Mechanical properties			
	Tensile E-modulus (MPa)	Compressive E-modulus (MPa)	Poisson ratio (-)	Density (kg/m^3)
Epoxy	[1]4500	[1]3000	[1]0.37	[5]1300
Acrylics	[1]100	[1]10	[2]0.45	[6]1200
Spruce (// fibers)	[3]11600	[4]550	[3]0.4	[7]440

Figure 1: Geometry of the double-lap joint.

and they were stored in a conditioning room for at least 1 week to obtain (a) a uniform moisture content of 12% and (b) fully cured adhesives.

2.2 Experimental procedure and instrumentation

The experimental program included both axial tensile and compressive experiments. The joint specimens were loaded up to failure at a displacement rate of 2 mm/min. In most of the specimens an unloading-reloading cycle was implemented (see below).

A universal Schenk machine of 600 kN capacity was used. Teeth-formed steel plates were installed to prevent both grip failure and slip of the specimens. The machine's load-cell and two LVDTs, symmetrically placed on both sides of the specimens at a distance of 330 mm, were used to measure the load and the displacements applied to the joints respectively, see Figure 2. The average values of the two LVDT measurements are reported in the following section.

In total, 11 specimens (5 epoxy and 6 acrylic ones) were examined in tension and 8 in compression (4 and 4 for each adhesive). The specimens were labeled according to the adhesive (E for epoxy or A for acrylic), the type of loading (T for tension or C for compression) and the number of the specimen, e.g. A_T2 denotes the second (2) acrylic (A) joint in tension (T).

3 RESULTS

3.1 Failure modes

Different failure modes were observed in tension and compression for the two types of joints, as summarized in Tables 2 and 3 and shown in Figures 3 and 4. All epoxy joints failed in the
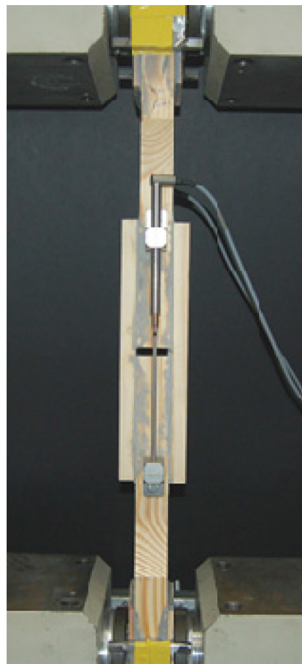

Figure 2: Experimental setup for tension and compression.

Table 2: Experimental results for joints in tension.

Speci-men	Initial stiffness K_I (kN/mm)	Yield load F_y (kN)	Yield displacement d_y (mm)	Ultimate load F_u (kN)	Ultimate displacement d_u (mm)	Failure mode
E_T1	131.34	-	-	32.21	0.24	adherend
E_T2	172.00	-	-	29.16	0.17	adherend
E_T3	231.99	-	-	47.07	0.19	adherend
E_T4	187.07	-	-	43.50	0.24	adherend
E_T5	197.61	-	-	33.68	0.17	adherend
AV ± SD	*184.00 ± 32.91*	-	-	*37.12 ± 6.91*	*0.20 ± 0.03*	
A_T1	126.03	39.00	0.33	56.58	3.04	mixed
A_T2	119.54	45.57	0.44	65.11	2.96	mixed
A_T3	99.42	41.00	0.47	61.64	2.95	mixed
A_T4	129.74	37.72	0.34	53.63	1.86	mixed
A_T5	139.38	40.76	0.32	65.80	3.47	adherend
A_T6	98.59	40.00	0.42	55.64	2.46	mixed
AV ± SD	*118.78 ± 15.17*	*40.68 ± 2.45*	*0.39 ± 0.06*	*59.73 ± 4.71*	*2.79 ± 0.51*	

Table 3: Experimental results for joints in compression.

Specimen	Initial stiffness K_I (kN/mm)	Yield load F_y (kN)	Yield displacement d_y (mm)	Ultimate load F_u (kN)	Ultimate displacement d_u (mm)	Failure mode
E_C1	118.75	-	-	53.93	0.49	adherend
E_C2	149.25	-	-	60.25	0.43	adherend
E_C3	128.30	-	-	64.89	0.55	buckling
E_C4	138.63	-	-	63.20	0.54	buckling
AV ± SD	*133.73 ± 28.75*	-	-	*60.57 ± 4.18*	*0.50 ± 0.05*	
A_C1	99.27	28.79	0.29	32.23	0.50	interfacial
A_C2	92.64	32.42	0.35	34.73	0.57	interfacial
A_C3	111.21	37.00	0.34	40.55	0.53	interfacial
A_C4	128.25	40.40	0.32	44.55	0.54	interfacial
AV ± SD	*107.84 ± 13.53*	*34.65 ± 4.41*	*0.33 ± 0.02*	*38.02 ± 4.83*	*0.54 ± 0.03*	

wood of the inner adherend (adherend failure), except for two of them in compression, which buckled during loading. The initiation of failure in tension occurred on the outer side just below the adhesive layer, while in compression initiation was at mid-height on the inner side.

A mixed failure mode was observed in the acrylic joints in tension; failure occurred partially in the wood and partially in the epoxy–acrylic adhesive interface on one side while on the other side failure occurred in the wood. In compression, failure occurred completely in the adhesive interface on one side and in the wood on the other side.
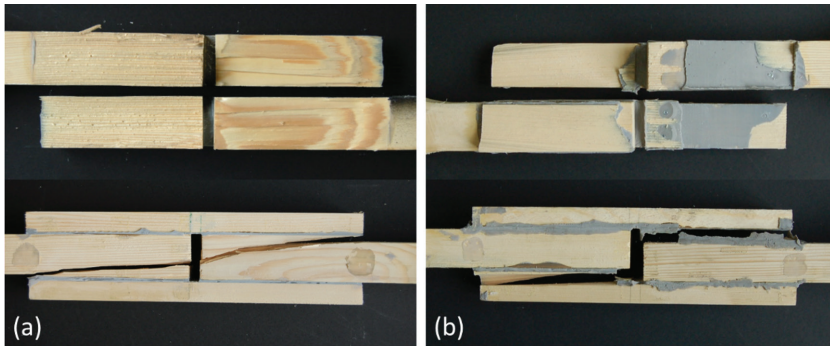
Figure 3: Failure modes in tension: (a) adherend failure for epoxy joints (E_T3) and (b) mixed failure for acrylic joints (A_T1), plan and side views.
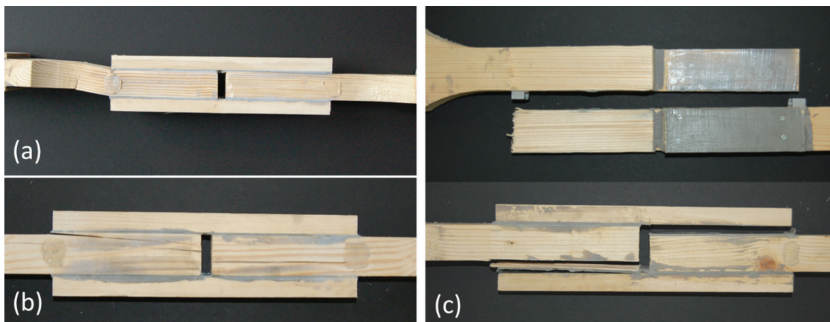

Figure 4: Failure modes in compression: (a) buckling (E_C4) and (b) adherend failure for epoxy joints (E_C1) and (c) interface failure for acrylic joints (A_C2).

3.2 Load–displacement responses

Typical load–displacement curves are shown in Figure 5. The responses were linear for the epoxy joints but highly non-linear for the acrylic ones. The unloading of the acrylic joints was performed at approximately 50 kN.

4 DISCUSSION

4.1 Mechanical characterization

Based on the Swiss code for timber structures [20] and the load–displacement curves shown in Figure 5, the joints were mechanically characterized, as described in Figure 6. The main mechanical properties included the initial stiffness, K_I, the yield load and displacement, F_y and d_y, and the ultimate ones, F_u and d_u, where failure occurred. The full set of the calculated properties are included in Tables 2 and 3.

The results showed that the epoxy joints exhibited a significantly stiffer initial behavior in tension and compression than the acrylic joints, while the latter showed a much higher deformation at failure in tension. In compression, the full deformation capacity
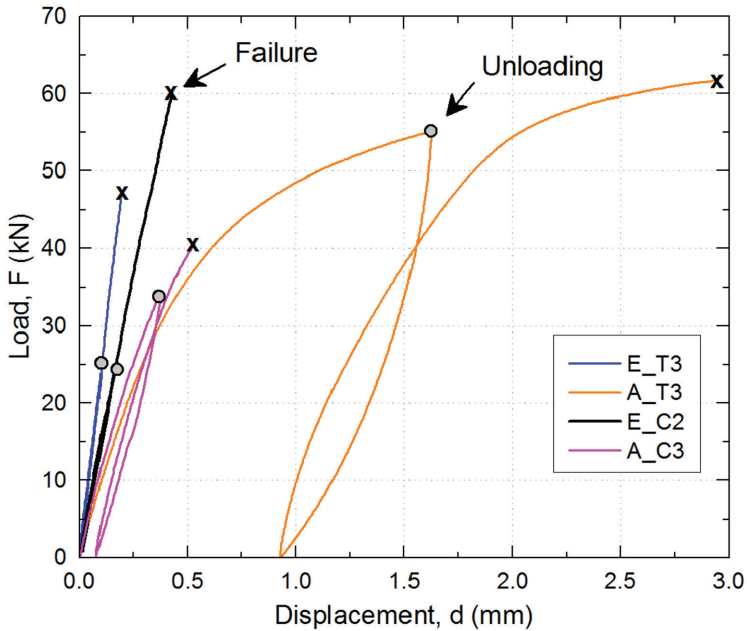
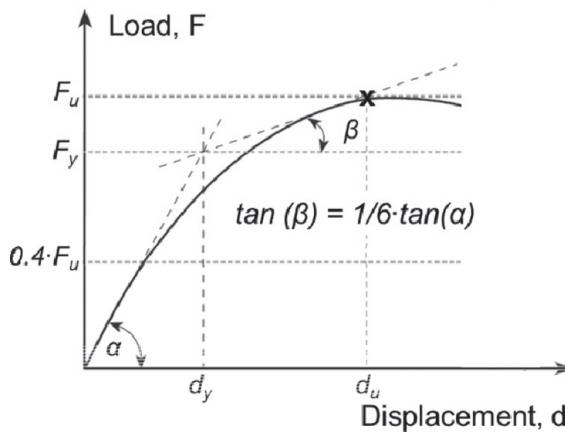Figure 5: Load–displacement responses of epoxy and acrylic joints in tension and compression.

Figure 6: Definition of stiffness and ductility (SIA265).

could not be developed due to the premature failure in the interface, as mentioned above. The highest and similar ultimate loads were obtained in the epoxy joints in compression and the acrylic joints in tension. The lower ultimate loads of the epoxy joints in tension may be traced back to the different location of failure initiation, as described above. The lower ultimate loads of the acrylic joints in compression were attributed to the interface failure.
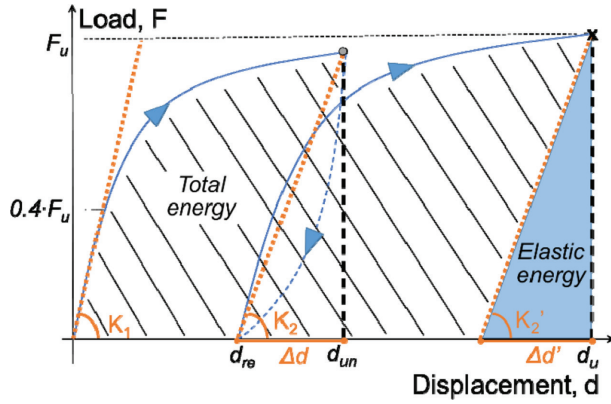
Figure 7: Definition of total and elastic energy.

4.2 Ductility of the joints

The deformation- and energy-based ductility indexes, μ_d and μ_e, as mentioned above, were calculated for the acrylic joints, as follows:

$$\mu_d = \frac{d_u}{d_y} \tag{1}$$

$$\mu_e = 0.5 \cdot \left(E_{tot} / E_{el} + 1 \right) \tag{2}$$

The energy-based index was selected according to Ref. [12] and the corresponding total energy, E_{tot}, and elastic energy, E_{el}, were determined, as shown in Figure 7. A difficulty in
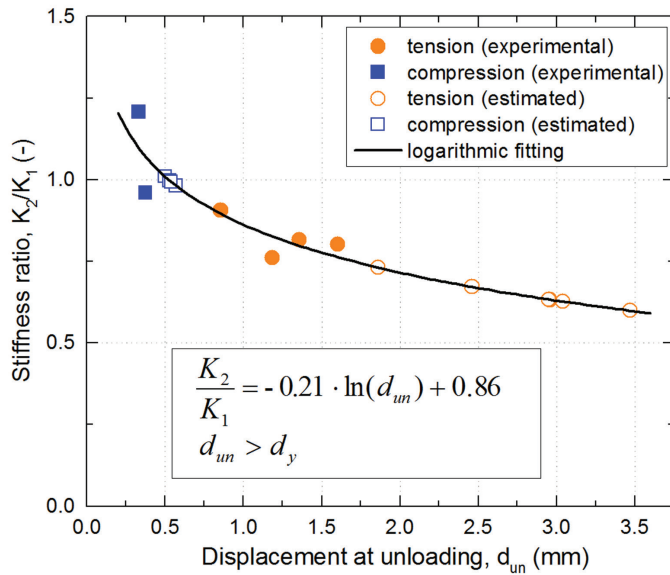

Figure 8: Relationship between stiffness ratio K_2/K_1 and displacement at unloading, d_{un}.

Table 4: Displacement- and energy-based ductility indexes of acrylic joints in tension.

| Specimen | Load at unloading F_{un} (kN) | Displacement at unloading d_{un} (mm) | Unloading stiffness, (kN/mm) | | Total energy E_{tot} (J) | Elastic energy E_{el} (J) | Displacement-based ductility μ_d (-) | Energy-based ductility μ_e (-) |
			Experimental K_2	Estimated K_2'				
A_T1	50.05	1.19	95.88	79.04	144.24	20.25	9.24	4.06
A_T2	-	-	-	75.65	154.61	28.02	6.73	3.26
A_T3	55.11	1.60	79.75	62.99	155.18	30.16	6.41	3.07
A_T4	-	-	-	94.88	78.46	15.16	5.47	3.09
A_T5	52.06	0.86	126.36	83.51	226.43	25.92	10.63	4.87
A_T6	49.74	1.36	80.49	66.26	98.40	23.36	5.33	2.61
AV ± SD	*51.74 ± 2.14*	*1.25 ± 0.27*	*95.62 ± 18.88*	*77.06 ± 10.64*	*142.89 ± 47.26*	*23.81 ± 5.00*	*7.30 ± 1.97*	*3.49 ± 0.75*

Table 5: Displacement- and energy-based ductility indexes of acrylic joints in compression.

| Specimen | Load at unloading F_{un} (kN) | Displacement at unloading d_{un} (mm) | Unloading stiffness (kN/mm) | | Total energy E_{tot} (J) | Elastic energy E_{el} (J) | Displacemen-based ductility μ_d (-) | Energy-based ductility μ_e (-) |
			Experimental K_2	Estimated K_2'				
A_C1	-	-	-	100.25	9.90	5.18	1.72	1.46
A_C2	-	-	-	90.98	12.36	6.63	1.64	1.43
A_C3	34.07	0.33	134.13	110.93	13.40	7.41	1.83	1.40
A_C4	35.28	0.38	122.93	127.42	15.70	7.79	1.68	1.51
AV ± SD	*34.68 ± 0.61*	*0.35 ± 0.02*	*128.53 ± 5.60*	*107.39 ± 13.55*	*12.84 ± 2.08*	*6.75 ± 1.00*	*1.72 ± 0.07*	*1.45 ± 0.04*

calculating this index was that the required unloading path just before failure could not be experimentally captured due to the scatter of the ultimate loads, see Tables 2 and 3. Unloading was thus performed earlier as described above and the unloading stiffness, K_2, as defined in Figure 7, was calculated. A logarithmic relationship between the stiffness ratio K_2/K_1 and the displacement at unloading, d_{un}, could then be established, see Figure 8. Based on this relationship, the stiffnesses of the unloading paths just before failure, K_2', i.e. at $d_{un} = d_u$, were estimated and μ_e was calculated based on these values, as shown in Tables 4 and 5. This procedure also allowed to estimate the indexes of the joints for which no cycles were performed.

The relationship between the displacement- and energy-based ductility indexes was linear, as shown in Figure 9. The much lower values of the prematurely failed specimens in compression also fitted into this result. The two indexes were further exponentially related to the ultimate displacement, as shown for the energy-based index in Figure 10.
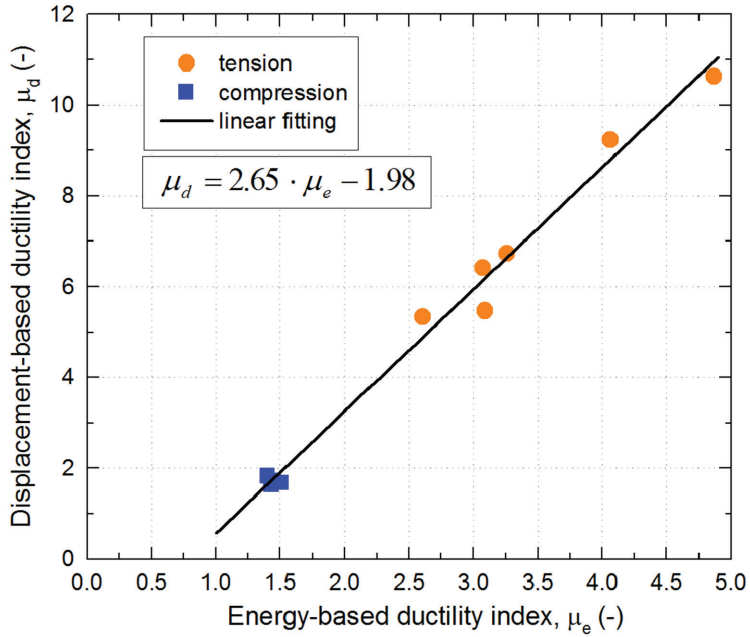
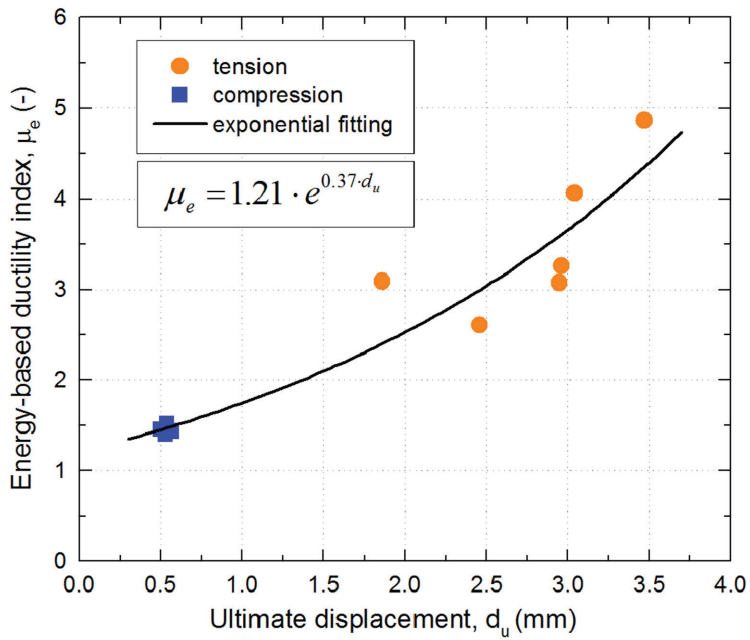Figure 9: Relationship between energy- and displacement-based ductility indexes.

Figure 10: Relationship between energy-based ductility index and ultimate displacement.

The displacement-based indexes in tension, 7.30 on average, are much higher than values given in timber codes for high ductility, e.g. Swiss code SIA265, where high ductility is assigned to values of μ_d >3.0. Considering the energy-based definition, the tension values, 3.49 on average, are also high compared to other materials (excluding metals), e.g. compared to 2.5 for glass-fiber-reinforced polymer (GFRP) bridge decks, adhesively-bonded onto steel girders [21], or prestressed concrete beams with unbonded FRP tendons subjected to bending, whose calculated ductility index was in the range of 2–5 [22].

5 CONCLUSIONS

Bonded double-lap timber joints have been studied in tension and compression, using two different structural adhesives; a brittle epoxy and a ductile acrylic adhesive. The main conclusions of this study can be summarized as follows:

- Epoxy-bonded joints exhibited a stiff linear load–displacement response. Failure occurred in the inner adherend, while the location of failure initiation in tension and compression was different and highly influenced the ultimate load, i.e. ultimate loads in compression were much higher than in tension.
- Acrylic-bonded joints showed a highly non-linear load–displacement response. A mixed failure mode was observed in tension; the ultimate loads reached the same high values as in the epoxy joints subjected to compression. Premature interface failure occurred in compression and thus reduced the joint capacity.
- Displacement- end energy-based ductility indexes were calculated for the acrylic joints. Subjected to tension, the joints exhibited high ductility compared to other materials and systems.

REFERENCES

[1] Tannert, T., Vallée, T. & Hehl, S., Temperature dependent strength of adhesively bonded timber joints. In *Proceedings of the International Conference on Wood Adhesives*, pp. 76–80. 2009.

[2] De Castro, J., *System ductility and redundancy of FRP structures with ductile adhesively-bonded joints.* EPFL, Lausanne, 2005.

[3] Lehmann, M., Vallée, T., Tannert, T. & Brunner, M., Adhesively bonded joints composed of wooden load-bearing elements. In *12th International Conference on Fracture*, ICF-12, pp. 2741–2749, Ottawa, ON, 2009.

[4] Tannert, T., Vallée, T. & Hehl, S., Experimental and numerical investigations on adhesively bonded hardwood joints. *International Journal of Adhesion and Adhesives*, **37**, pp. 65–69, 2012.
https://doi.org/10.1016/j.ijadhadh.2012.01.014

[5] Keller, T. & De Castro, J., System ductility and redundancy of FRP beam structures with ductile adhesive joints. *Composites Part B: Engineering*, **36**(8), pp. 586–596, 2005.
https://doi.org/10.1016/j.compositesb.2005.05.001

[6] Banea, M.D. & da Silva, L.F.M., Mechanical characterization of flexible adhesives. *Journal of Adhesion*, **85**(4–5), pp. 261–285, 2009.
https://doi.org/10.1080/00218460902881808

[7] Park, R. & Pauley, T., *Reinforced Concrete Structures*, John Wiley and Sons: New York, United States of America, 1975.
https://doi.org/10.1002/9780470172834

[8] Baker, J.F, Horne, M.R. & Heyman, J., *Plastic Behavior and Design, the Steel Skeleton, vol.2*, UK: Cambridge University Press, 1956.

[9] Yanes-Armas, S., de Castro, J. & Keller, T., Energy dissipation and recovery in web-flange junctions of pultruded GFRP decks. *Composite Structures*, **148**, pp. 168–180, 2016.
https://doi.org/10.1016/j.compstruct.2016.03.042

[10] Grace, N.F., Soliman, A., Abdel-Sayed, G. & Saleh, K., Behavior and ductility of simple and continuous FRP reinforced beams. *Journal of Composites for Construction*, **2**(4), pp. 186–194, 1998.
https://doi.org/10.1061/(ASCE)1090-0268(1998)2:4(186)

[11] De Lorenzis, L., Galati, D. & La Tegola, A., Stiffness and ductility of fibre-reinforced polymer-strengthened reinforced concrete members. *Proceedings of the Institution of Civil Engineers - Structures and Buildings*, **157**(1), pp. 31–51, 2004.
https://doi.org/10.1680/stbu.2004.157.1.31

[12] Naaman, A.E. & Jeong, S.M., Structural ductility of concrete beams prestressed with FRP tendons, Nonmetallic (FRP) reinforcement for concrete structures. *Proceeding of the Second International RILEM Symposium (FRPRCS-2),* pp. 379–386, 1995.

[13] Vallée, T., Tannert, T. & Hehl, S., Ductile adhesively bonded timber joints. *Wood Adhesives, Session 4B*, pp. 315–318, 2009.

[14] Sika, A.G., SikaDur-330: 2-part epoxy impregnation resin, 2006.

[15] Sika, A.G., SikaFast5221 NT: Fast-curing 2-component structural adhesive. *Zurich*, 2013.

[16] Angelidi, M., Vassilopoulos, A.P. & Keller, T., Ductility, recovery and strain rate dependency of an acrylic structural adhesive. *Construction and Building Materials*, **140**(1), pp. 184–93, 2017.
http://dx.doi.org/10.1016/j.conbuildmat.2017.02.101

[17] Angelidi, M., Vassilopoulos, A.P. & Keller, T., Displacement rate and structural effects on Poisson ratio of a ductile structural adhesive under tension and compression. *International Journal of Adhesion and Adhesives*, 2016.

[18] Dinwoodie, J.M., Timber - a review of the structure-mechanical property relationship. *Journal of Microscopy*, **104**(1), pp. 3–32, 1975.
https://doi.org/10.1111/j.1365-2818.1975.tb04002.x

[19] Zhong, W., Huang, X., Hao, Z., Hu, W., Zhou, H. & Chen, G., Investigation of compressive properties of spruce along spatial different loading orientations. *15th International Conference on Experimental Mechanics*, Porto, 2012.

[20] SIA. 265–Timber structures, Swiss Standards Association, 2003.

[21] Keller, T. & Gürtler, H., Composite action and adhesive bond between FRP bridge decks and main girders. *Journal of Composites for Construction*, **9**(4), pp. 360–368, 2005.
https://doi.org/10.1061/(ASCE)1090-0268(2005)9:4(360)

[22] Jo, B.W., Tae, G.H. & Kwon, B.Y., Ductility evaluation of prestressed concrete beams with CFRP tendons. *Journal of Reinforced Plastics and Composites*, **23**(8), pp. 843–859, 2004.
https://doi.org/10.1177/0731684404033492